# Effect of Parameters on Fiber Diameters and the Morphology of Hybrid Electrospun Cellulose Acetate/Chitosan/Poly(Ethylene Oxide) Nanofibers

***Salehizadeh, Pantea; Taghizadeh, Masoud****[+]

*Department of Food Science and Technology, Ferdowsi University of Mashhad (FUM), Mashhad, I.R. IRAN*

***Emam-Djomeh, Zahra****[+]

*Department of Food Science, Technology and Engineering, Faculty of Agricultural Engineering and Technology, University College of Agriculture and Natural Resources, University of Tehran, Karaj, I.R. IRAN*

**ABSTRACT:** *Electrospun NanoFibers (ENFs) were fabricated from the mixture of Cellulose Acetate (CA), chitosan (CHI), and poly (ethylene oxide) using an acetic acid solution. The impact of CA/CHI ratio (0.5, 1, 1.5 wt %), CHI/PEO ratio (1, 1.5, 2 wt%), Sodium Dodecyl Sulfate (SDS) (0, 1.5, 3% w/w) and ammonium oxalate (3%, w/w) on the diameter, tensile strength, elongation, and porosity of the ENFs were optimized using Response Surface Methodology-Central Composite Rotatable Design (RSM-CCRD). The results revealed that ENFs were formed of non-woven fibers with a maximum diameter of 113 nm. Second-order polynomial models with high $R^2$ values (0.996–0.99) were developed using Cubic analysis. The optimum condition was identified to be at the compounded level of CA/CHI 1.5 wt%, CHI/PEO 1 wt%, and SDS 3% (w/v). At the best point, the diameter, surface tension, elongation, and porosity of the fabricated ENFs were 96.07 nm, 0.054 N/mm$^2$, 13.09 mm, and 52.29 respectively.*

**KEYWORDS:** *Electrospinning; Cellulose acetate; Chitosan; Fiber diameter; Morphology*.

## INTRODUCTION

Electrospinning is considered novel processing, producing polymeric fibers in a range of micro to nanometers. Some processing techniques can prepare nanofibers, including self-assembly [1], template synthesis [2], electro-spinning [3], drawing [4], and phase separation [5]. The drawing can make one-by-one long single nanofibers; however, a viscoelastic material just can suffer strong deformations. The template synthesis needs a nanoporous membrane as a template to make nanofibers of solid or hollow shape. The phase separation takes a fairly long time to transfer the solid polymer into the nano-porous foam. This technique includes extraction, gelation, and dissolution using drying, freezing, and a different solvent resulting in a nanoscale porous foam. The self-assembly, the same as the phase separation is a time-consuming process and in its individual components organize themselves into desired functions and patterns. Hence, the electrospinning process seems to be the only

***** *To whom correspondence should be addressed.*
*+ E-mail: mtaghizadeh@um.ac.ir ; emamj@ut.ac.ir*
*1021-9986/2022/8/2537-2547 11/$/6.01*

method, which can be further developed for the mass production of continuous nanofibers from various polymers. Electrospun NanoFibers (ENFs) have great properties such as mechanical performance, high porosity, and flexibility that can be applied in varieties applications such as food packaging [6], enzyme immobilization [7], therapy and regeneration of damaged and nerve tissue [8, 9], wound healing [10] and air and water filtration system [11].

Cellulose Acetate (CA) is a renewable abundant polymer with exceptional tensile strength, stiffness, renewability, biodegradable and biocompatible, low-cost, and notable flexibility [12, 13]. However, electrospinning of cellulose would be a complicated process due to the low solubility of CA in traditional solvents, and could not melt due to a great deal of intermolecular hydrogen bonding [14]. Chitosan is another abundant natural biopolymer with high functional groups. Chitosan is polycationic in aqueous acidic solvents and has amino groups in its polymer backbone that this strong chain interaction between the iconic groups in the polymer lead to an increase in viscosity and surface tension of the spinning solution [15]. Chitosan nanofibers have poor chemical, thermal, and mechanical stability and swell excessively in water leading to reduce mechanical strength and making them unstable for filtration [16].

Condition of electrospinning, polymer solutions, and mixing with other polymers could offer a wide variety of approaches for the fabrication of amazing electrospun nanofibers properties [17]. The adsorptive blend hollow fiber membranes were produced from CA & CHI, as CA has excellent mechanical properties and primary amine (-$NH_2$) and hydroxy (-OH) in chitosan and hydroxyl (OH) groups in CA can be better reaction groups for Sorption metals [16]. The mechanical properties including tensile strength and elongation of polymer nanofibers lead to generating the point-bonded structures (due to the adhesive), that increase the number of potential applications of mechanically weak electrospun nanofibers [18].

The main challenge of making polymers from these two polymers is to find the right solution. The previous study showed that CA/CHI could not be fabricated from acetic acid /acetone, but Cellulose and dibutyl chitin (DBC) (chitosan ester) hybrid were generated nanofibers, using 1/1 acetone/acetic acid solvents resulting 30-350 nm fiber diameters [19]. The uniform average 450 nm fiber was fabricated from cellulose acetate/chitosan 60:40 from binary co-solvent including 70:30 trifluoracetic acid (TFA); methylene chloride (DCM) [17]. However, TFA is an expensive, volatile, and toxic solvent. The research showed that Cellulose monoacetate/chitosan-blended nanofibers could be fabricated using acetone, which has a high evaporation rate that would consider a disadvantage of this solvent [7].

Introducing additives such as poly (ethylene oxide) (PEO) or poly (vinyl alcohol) (PVA) in solution could actively interfere with chitosan through hydrogen bonding on the molecular level leading to an increase in the production of chitosan nanofibers with lower fiber diameters [20]. The addition of salt and surfactant could increase the viscosity and conductivity and decrease the surface tension of the solution, which is essential for the total suppression of the beads [12, 21].

Therefore, the aim of this study is to fabricate great potential ENFs by blending two biopolymers CA/CHI ENFs by adding PEO, ammonium oxalate, SDS and using the acetic acid as a non-toxic solvent. Besides, the ENFs were characterized in terms of their morphology and mechanical properties including tensile strength and elongation, and finally, blended ENFs would compare with CA/PEO and CHI/PEO ENFs.

## EXPERIMENTAL SECTION

### *Materials*

Chitosan (low molecular weight, Mw = 50–190 kDa; the degree of deacetylation, DDA = 75–85%) and polyethylene oxide (PEO) (Mn = 200 kDa) and cellulose acetate CA (Mn = 30 kDa, 39.8 wt% acetyl content) were obtained from Sigma Chemical Co. (St. Louis, MO, USA). Acetic acid 90%, ammonium oxalate $C_2H_8N_2O$, and Sodium dodecyl sulfate were purchased from Merck Chemical Co. (Darmstadt, Germany).

### *Solution preparation*

The fixed polymer proportion and a determined amount of ammonium oxalate and sodium dodecyl sulfate (Table1) in acetic acid 90%, according to CCRD, were dissolved and stirred for 24h at an ambient temperature under a constant stirring rate (300 ± 1 rpm) to obtain the clear and homogenous solutions then kept in sealable brown bottles at room temperature (23 ± 2 °C). The total polymer ratio in the solvents was 4.8% (w/v). In this experiment, solutions of CA/PEO 7% (w/v) and CHI/PEO

***Table 1: The central composite rotatable design (CCRD) matrix and experimental data obtained for the response variables (mean ± SD). FD: Fiber Diameter, PO: Porosity, TS: Tensile strength, EB: Elongation at Break.***

| Run | CA/CHI | CHI/PEO | SDS | FD | PO | TS | EB |
|---|---|---|---|---|---|---|---|
| | w/w% | w/w% | wt% | nm | (%) | ($N/mm^2$) | mm |
| 1 | 0.5 | 1 | 3 | 100 | 48.07 | 0.05 | 7.60 |
| 2 | 1 | 2 | 1.5 | 98 | 40.32 | 0.04 | 12.64 |
| 3 | 1.5 | 2 | 3 | 89 | 47.05 | 0.03 | 11.49 |
| 4 | 1 | 1.5 | 1.5 | 101 | 61.80 | 0.04 | 12.88 |
| 5 | 1 | 1.5 | 1.5 | 102 | 61.93 | 0.04 | 11.99 |
| 6 | 0.5 | 1.5 | 1.5 | 100 | 37.11 | 0.02 | 19.55 |
| 7 | 1 | 1.5 | 1.5 | 99 | 62.70 | 0.03 | 12.01 |
| 8 | 1.5 | 2 | 0 | 109 | 64.17 | 0.03 | 6.13 |
| 9 | 1 | 1.5 | 1.5 | 101 | 61.80 | 0.04 | 12.88 |
| 10 | 1.5 | 1.5 | 1.5 | 94 | 49.87 | 0.06 | 6.20 |
| 11 | 1 | 1.5 | 0 | 104 | 47.30 | 0.06 | 6.25 |
| 12 | 0.5 | 2 | 3 | 111 | 67.68 | 0.01 | 17.58 |
| 13 | 1.5 | 1 | 3 | 95 | 52.68 | 0.06 | 12.88 |
| 14 | 1 | 1.5 | 3 | 119 | 75.18 | 0.03 | 5.82 |
| 15 | 1 | 1.5 | 1.5 | 101 | 58.30 | 0.04 | 12.80 |
| 16 | 1.5 | 1 | 0 | 111 | 61.80 | 0.05 | 7.15 |
| 17 | 0.5 | 2 | 0 | 109 | 65.80 | 0.01 | 19.34 |
| 18 | 1 | 1.5 | 1.5 | 98 | 60.53 | 0.04 | 12.98 |
| 19 | 0.5 | 1 | 0 | 113 | 69.55 | 0.04 | 6.13 |
| 20 | 1 | 1 | 1.5 | 104 | 49.15 | 0.03 | 14.00 |

4.8% (w/v) with the same conditions for comparison with the blended CA/CHI/PEO prepared.

***Electrospinning of CA/CHI/PEO solutions***

Electrospinning was performed using a 1 mL syringe fitted with a blunt-ended metal needle (22 gauge, 0/7mm) at a 17–23 kV voltage in horizontal alignment. The polymer solution was placed in a syringe pump operated at 0.0033-0.0066 mL $min^{-1}$ with a needle tip-to-collector distance of 10-23 mm. Fibers were collected on aluminum foil covered on the drum and detached from the collector to be analyzed with Scanning Electron Microscopy (SEM).

***Analytical methods***

*Elongation and Tensile strength*

Elongation and Tensile strength were tested using Brookfield CT3 Texture Analyzer. The size of the sample was 50 mm in height, 15 mm in width, and 10 mm in thickness. The experiment was carried out in three replicates (Texture CT V1.8 Build 31, USA).

*Porosity measurement*

The porosity of the ENFs was determined using Image J and obtained histograms from SEM images. This method of the image can analyze the porosity of nanofibers through SEM images. In this process, the upper and lower

layers can be identified according to their intensity region, by calculating the threshold (Eq. ()), we can classify different layers of nanofibers by converting the original image to binary form, and the porosity in each binary image can be calculated using the mean intensity of images (eq.2) as follows:

$$1.\ \text{Threshold 1: } (\mu + \text{б})/255 \quad (1)$$

$$2.\ \text{Threshold 1: } \mu/255$$

$$1.\ \text{Threshold 1: } (\mu - \text{б})/255$$

Where $\mu$ is the mean and $б$ standard deviation of the image matrix (Eq.(1)). The first threshold eliminates lower layers and only the surface layers are obtained, the second threshold can represent the sum of surface and middle layers, and the third threshold illustrates all of the visible layers.

$$P = \left(1 - \frac{n}{N}\right) \times 100 \quad (2)$$

Where *P* is the porosity percentage of the binary image, *n* is the number of white pixels, *N* is the total number of pixels in the binary image [22].

***Morphology of CA/CHI/PEO ENFs***

The morphologies of CA/CHI/PEO ENFs were evaluated with a low and high magnification (KYKY-EM3200 SN: 0056) scanning electron microscope (SEM). At first, Samples were mounted on an SEM sample holder and sputtered with gold-palladium (thickness of 100A˚) with a BAL-TEC SCD005 sputter coater (BAL-TEC AG, Balzers, Liechten- stein. The average diameter of each SEM fiber image was studied by Image J software (Mac version; 2.0.0-RC-43/1.50e) with a hundred measurements.

***Experimental design and statistical analysis***

RSM-CCRD was applied for the optimization of the reaction conditions. This approach was carried out to assess the effect of the three first independent variables consist of the Cellulose Acetate (CA) /chitosan (CHI) ratio ($X_1$, 0.5–1.5 wt.%), chitosan/polyethylene oxide (PEO) ratio ($X_2$,1–2 wt.%), Sodium Dodecyl Sulfate (SDS) ($X_3$, 0, 1.5, 3% w/w) on the diameter, tensile strength, elongation, and porosity. This fabrication of ENFs was improved using response surface methodology-central composite rotatable design (RSM-CCRD) [18] and a Cubic model CCRD (Table 1), 20 solutions of bicomponent polymer were prepared. The center point was repeated six times to estimate the repeatability of the method [23]. The response functions (y) were related to the coded variables (Xi, i = 1, 2) by a second-order polynomial using the following equation:

$$Y = \beta_0 + \beta_1 x_1 + \beta_2 x_2 + \text{ß}_{12} x_1 x_2 + \beta_{11} x_{21} + \beta_{22} x_{21} \quad (1)$$

The coefficients of the polynomial equation equaled to $ß_0$ (constant term), $ß_1$, $ß_2$, and $ß_3$ (linear effects), $ß_{11}$, $ß_{22}$ and $ß_{33}$ (quadratic effects) and $ß_{12}$, $\beta_{23}$, $\beta_{123}$, $\beta_{112}$, $\beta_{113}$ and $\beta_{122}$ (interaction effects). The quality of the fit of the cubic model polynomial model was described as the coefficient of determination $R^2$, adjusted $R^2$ ($R^2$ adj), predicted $R^2$ ($R^2$-perd), and adequate precision (ADP). ADP compares the range of the predicted values at the design points to the average prediction error. A ratio greater than 4 is desirable. The design was constructed with the Design Expert statistical package (version 12 DESIGN-EXPERT, Minneapolis, MN, USA). Analysis of variance (ANOVA) was carried out to study the fitness of the constructed models and to determine the significant factors. All experiments were analyzed at the same time due to minimizing the effect of experimental errors in the observed responses.

## RESULTS AND DISCUSSION

***Characterization of CA/CHI/PEO blend solutions***

Some experiments were carried out to achieve suitable conditions for producing ENFs (data has not been shown). The results depicted that the dependent and independent variables were suitably fitted by the second-order polynomial equation. The statistical significance, the linear and quadratic equations, cubic, and the interaction effects assessed for each response are brought in Table 2. The 3D and perturbation plots for the combined effect of CA/CHI, CHI/PEO, and SDS content on diameter, tensile strength, elongation, and porosity of the fabricated nanofiber were shown in Fig. 1. These plots illustrate that the response changes as each factor changes from the chosen reference point, with all other factors, held constant at the reference value. The findings depicted how the structure and morphology of the ENFs were undoubtedly affected by the ratio of CA/CHI, CHI/PEO, and SDS content.

***Porosity***

According to Table 2, the proposed porosity model was not significant 0.37, and the lack of fitness was P >0.05.

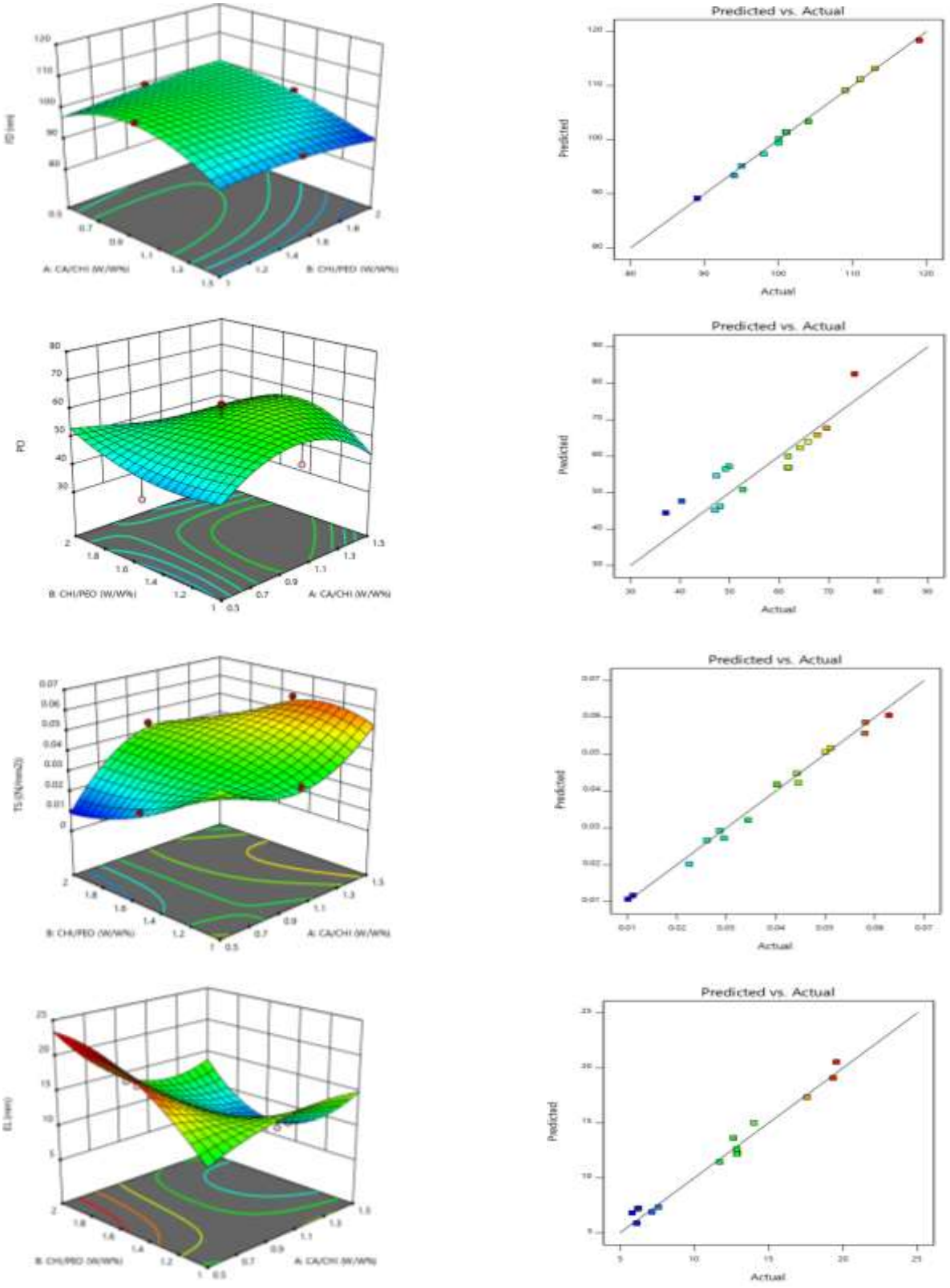


***Fig. 1: 3D graphs and predicted vs. actual plots illustrating the combined impact of cellulose acetate CA/CHI ratio, CHI/PEO ratio, SDS on the diameter (a), porosity (b), tensile strength (c), and elongation (d).***

***Table 2: ANOVA analysis of experimental variables as a linear, quadratic, and interaction terms of each response variable and corresponding coefficients for the predictive models.***

| Source | | FD (nm) | | PO | | TS ($N/mm^2$) | | EB (mm) | |
|---|---|---|---|---|---|---|---|---|---|
| | df | Sum of Squares | p-value | Sum of Squares | p-value | Sum of Squares | p-value | Sum of Squares | p-value |
| Model Linear | 13 | 962.19 | < 0.0001 | 1471.33 | 0.37 | 0.0038 | 0.0001 | 354.52 | 0.001 |
| β1 | 1 | 18.00 | 0.0016 | 81.45 | 0.36 | 0.0006 | 0.0001 | 89.11 | 0.0003 |
| β2 | 1 | 18.00 | 0.0016 | 38.98 | 0.51 | 0.0001 | 0.045 | 0.93 | 0.46 |
| β3 | 1 | 112.50 | < 0.0001 | 388.66 | 0.07 | 0.0006 | 0.0002 | 0.09 | 0.81 |
| Quadratic | | | | | | | | | |
| β11 | 1 | 70.01 | < 0.0001 | 100.34 | 0.31 | 0.0000 | 0.07 | 7.64 | 0.07 |
| β22 | 1 | 3.01 | 0.0667 | 63.28 | 0.42 | 0.0001 | 0.04 | 12.25 | 0.03 |
| β33 | 1 | 245.82 | < 0.0001 | 376.97 | 0.08 | 0.0000 | 0.26 | 73.55 | 0.0004 |
| Interaction | | | | | | | | | |
| β12 | 1 | 28.13 | 0.0005 | 45.64 | 0.48 | 0.0000 | 0.061 | 80.49 | 0.0003 |
| β13 | 1 | 78.13 | < 0.0001 | 5.49 | 0.80 | 1.646E-08 | 0.96 | 16.78 | 0.016 |
| β23 | 1 | 15.13 | 0.0024 | 29.48 | 0.57 | 0.0000 | 0.09 | 1.43 | 0.37 |
| β123 | 1 | 45.13 | 0.0001 | 122.90 | 0.27 | 1.001E-06 | 0.74 | 1.18 | 0.41 |
| β112 | 1 | 13.23 | 0.0034 | 57.42 | 0.44 | 0.0007 | < 0.0001 | 17.49 | 0.01 |
| β113 | 1 | 286.22 | < 0.0001 | 619.09 | 0.03 | 0.0005 | 0.0002 | 4.04 | 0.15 |
| β122 | 1 | 0.62 | 0.35 | 146.19 | 0.23 | 0.0002 | 0.0020 | 41.23 | 0.002 |
| Residual | 6 | 3.61 | 0.6011 | 496.39 | 82.73 | 0.0000 | 8.122E-06 | 9.17 | 1.53 |
| Total | 19 | 965.80 | | 1967.71 | | 0.0039 | | 363.69 | |

Therefore, these findings showed that the different ratios of CA/CHI/PEO content and SDS would not affect porosity (Fig.1b). However, there is a significant difference among different ENFs made of CHI/PEO, CA/PEO, and CA/CHI/PEO. As depicted in Table 3, CA/PEO nanofiber has the highest porosity than CA/CHI/PEO and CHI/PEO ENFs, respectively. It means that the higher fiber diameter, including higher porosity. *Ghasemi Mobarakeh et al.* [24] reported that the number of layers determines the porosity percentage, so raising the number of layers due to more fibers overlapping each other leads to a minimum value. Hence, the more layers, the less porosity percentage ENFs have. The result showed that CHI ENFs had the lowest porosity percentage due to having the smallest nanofiber diameter.

***Table 3: Comparison of the effects of different ENFs on fiber diameter, porosity, tensile strength, and elongation at Break (mm).***

| ENFs | FD (nm) | PO (%) | TS ($N/mm^2$) | EB (mm) |
|---|---|---|---|---|
| CA/CHI/PEO | 103.1 | 57.15 | 0.038 | 11.50 |
| CA/PEO | 138 | 77.64 | 0.017 | 3.93 |
| CHI/PEO | 61.46 | 49.01 | 0.012 | 5.26 |

***Tensile strength***

Adequate mechanical strength is needed for many nanofibers' applications. Therefore, the lack of nanofibers' toughness and strength would lead to a challenge in using them in different applications. As the fine fiber dimensions are sensitive to control, it is better to support one another in the nanofibers mat. The strength of ENFs is dependent on many points, like fiber diameter, length and orientation in the structure of the mat, fiber strength, fiber surface morphology, and the frictional cohesion forces among the fibers. In this study, the results showed that

blending chitosan with cellulose acetate enhanced tensile strength. This blended nanofiber needed 2.23, and 3.02 folds more forces to break toward CA/PEO and CHI/PEO nanofibers in the tensile test due to strong intermolecular interaction and CA/PEO nanofiber needed 1.42 N/mm$^2$ more than CHI/PEO to break (Table 3). As considered in Table 2, the suggested model for Tensile Strength (TS) was perfectly significant ($P < 0.0001$). The lack of fitness ($P > 0.05$) was not significant. Lack of fitness describes model divergence from the degree of generated predicted and experimental values. Hence, a non-significant lack of fitness implies the fitness of the model [25]. The ADP value was 20.92, which depicted a great signal-to-noise ratio for the experiment models. The tensile strength was highly affected by the ratio of CA/CHI ($X_1$; $P < 0.0001$), CHI/PEO ($X_2$; $P<0.05$) and related to the linear effect of SDS content ($X_3$; $P<0.0002$) (Table 2). The outcomes depicted that the quadratic of CHI/PEO ($P > 0.0372$) and the interaction of linear CA/CHI ratio with quadratic CHI/PEO was significant. Moreover, the mutual interaction of the quadratic CA/CHI ratio with CHI/PEO and SDS content was highly significant ($P<0.0001$) and ($P< 0.0002$), respectively. As shown in Fig.1c tensile strength increased by raising the CA/CHI ratio concentration and decreased with increasing CHI/PEO ratio and SDS concentration. SDS decreased the surface tension and led to smooth fibers, so the tensile strength decreased. The tensile strength of CHI fibers improved with combining with cellulose acetate. For decades, nanocellulose is stand out due to its mechanical unique rheological, and optical properties. The incorporation of nanocellulose in polymer matrices, even at low concentrations, could impart higher stiffness to the nanocomposites. This characteristic is because of its ability to produce interconnected network structures *via* hydrogen bonding [26].

The $R^2$ value for the tensile strength equation was 0.99. This result shows that the model could not evaluate only 1 % of the total variation. The values of Adj-$R^2$, Pred-$R^2$, CV, and ADP for this response were 0.96, -14.37, 7.38, and 20.92 respectively, which demonstrate the significant constructed model. The fitted equation to predict tensile strength behavior was brought in the following equation:

$$TS\ (N/mm^2) = 0.0417+0.01775X_1+ 0.00507X_2-0.0167X_3-0.00458X_{22}-0.021X_{12}X_2+0.0178X_{12}X_3-0.01169\ X_1X_{22}$$

***Elongation***

Table 2 shows that the suggested model for elongation value was highly significant ($P < 0.0001$) with a non-significant lack of fitness ($P > 0.05$). The values of the $R^2$ (0.97), Adj-$R^2$ (0.92), and Pred-$R^2$ (-29.99) proved that the model was highly significant. The break elongation of the three types of nanofibers is summarized in Table 3. Break elongation is explained as the extension per gauge length at the break. The findings demonstrated that the mixed nanofibers showed the highest length of the break. The elongation value of the CA/CHI/PEO blend nanofibers appears to be highly greater than that of CA/PEO and CHI/PEO ENFs. Elongation was attributed to the linear effect of CA/CHI concentration ($P<0.0003$). Although the quadratic effect of CHI/PEO and SDS concentration was not significant, the quadratic effect of CHI/PEO ratio and SDS concentration $P< 0.05$, the interaction among the ratio of CA/CHI & CHI/PEO and CA/CHI & SDS concentration were significant at $P< 0.05$. The interaction between the quadratic of CA/CHI and CHI/PEO concentration and the interaction between CA/CHI and the quadratic of CHI/PEO was $P < 0.002$. However, the interaction of all three values and the interaction between the quadratic of CA/CHI and the CHI/PEO were not significant. ADP and CV values were 14.18 and 10.74, which displays a good signal-to-noise ratio for the studied models. The fitted equation to predict Elongation behavior was brought in the following equation:

$$EL\ (mm)= 12.2081-6.675X_1-3.17191X_1X_2+ 1.44847X_1X_3+ 2.11097X_{22}-5.17167X_{32}+3.30637\ X_{12}X_3+5.07603\ X_1X_{22}$$

As illustrated in Fig.1d, by increasing CHI/PEO ratio, the elongation break increased; however, raising in CA/CHI ratio did not change significantly. As it is observed in table 3, the length of the elongation break of CA/CHI/PEO nanofiber is 2.94 and 2.18 mm more than CA/PEO and CHI/PEO nanofibers respectively. Hence, combining CA polymer with CHI improves its elongation due to the flexibility of CHI. However, CA/PEO nanofiber showed the least elongation break, due to CA nanofiber being stiff, so the length of the elongation break is low.

***Morphology of electrospinning fiber structures***

The polymer concentration, the molecular weight, and different surfactant percentages are three factors that can change fiber diameters [27]. *Zhang* and *Hsieh* [23]

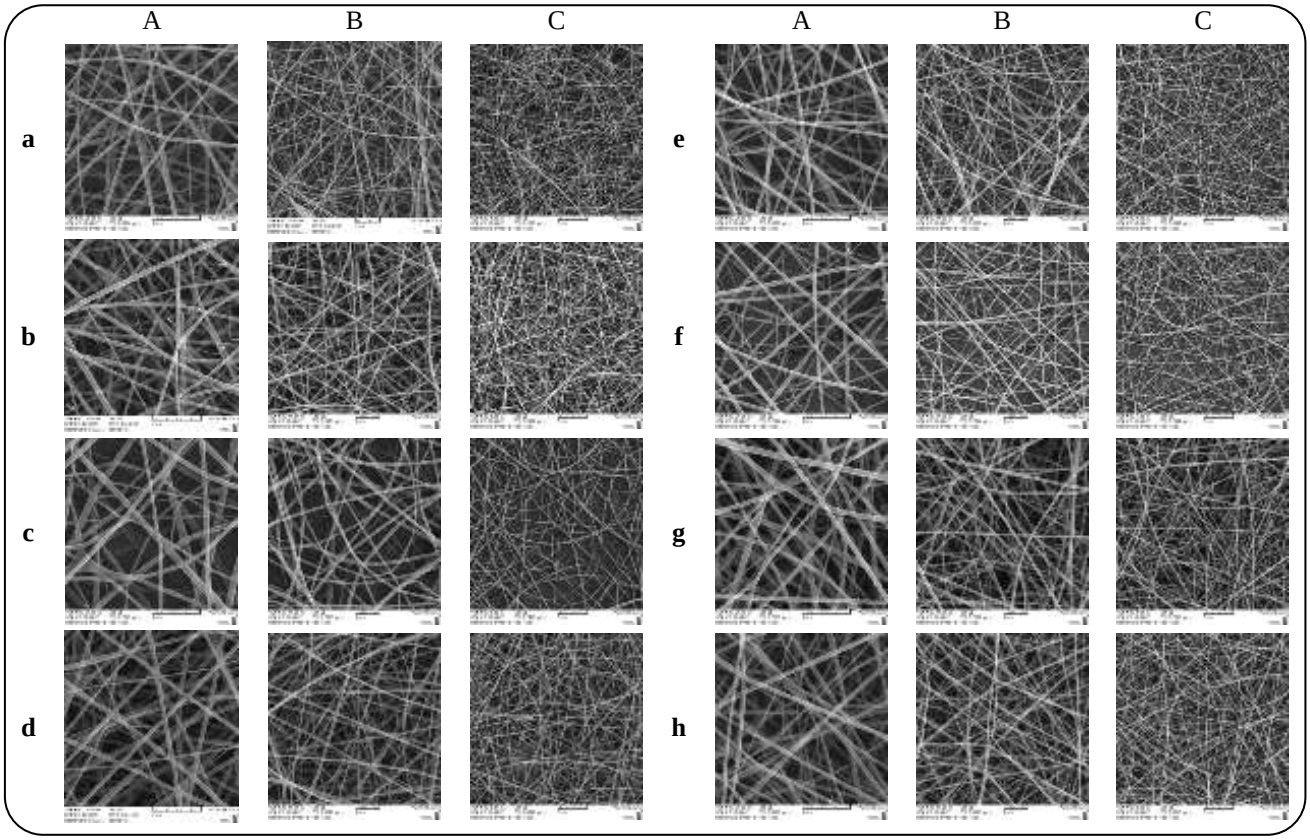


***Fig. 2: SEM micrographs of nanofibers with various contents of CA/CHI/PEO ratio and SDS%, (a) (run 10), (b) (run 2), (c) (run 16), (d) (run 13), (e) (run 3), (f) (run 8), (g) (run 20), (h) (run 11); different magnifications, 20 Kx (A), 10 Kx (B) & 5 Kx (C).***

reported that the chain length of polymers, mixing ratios, and the used solvent could influence the fabrication of fiber. In this study, a great SEM image was formed from Run 13 (CA/CHI: 1.5 wt%; CHI/PEO: 1 wt%; SDS content of 3% (w/v) produced uniform and bead-free electrospun fibers with diameter distribution between 89 to 119 and an average diameter of 96.07nm (Fig. 2d). Rising the SDS concentration from 0 to 3% (%w/w) decreased the surface tension leading to a decrease in the diameter of the fibers as *Jia* and *Qin* [28] found the same result. The finer ENFs were fabricated from ionized solutions with a higher ratio of CA/CHI ($P<0.001$), CHI/PEO, and SDS ratio ($P<0.0001$) (Fig.1a; Table 1). The finer fiber might be due to the high CHI/PEO ratio concentration and SDS of the initial solution (run 3) (Fig. 2e). Most nanofiber images showed a well-defined structure with no junction zone except in Fig. 2c. It showed that a high CA/CHI ratio and low SDS led to the junction zone, resulting better mechanical properties due to the reduction in surface-to-volume ratio. Increasing the solutions' conductivity could raise the formation of junction zone in the ENFs. The amount of surfactant is important due to after saturation of the polymer–surfactant begins to form the free surfactant micelles [29]. The introduced anionic and cationic surfactants interacted strongly with the hydrophobic groups of the polymer (Alkyl groups) caused to a strong association between polymer chains strongly [28]. Therefore in this experiment, SDS as an anionic surfactant is used to bring strong interaction in polymer chains and decrease surface tension because of the higher conductivity and lower surface tension.

Table 2 illustrates that the ENFs diameter significantly is attributed to the CA/CHI & CHI/PEO concentration ($P<0.001$). The diameter was directly affected by the linear effect of SDS concentration ($P<0.0001$). Although the quadratic effect of CHI/PEO concentration was not significant, the quadratic effect of CA/CHI ratio and SDS concentration, the interaction among the ratio of CA/CHI & CHI/PEO and SDS concentration were significant at $P<0.0001$. Moreover, the interaction between the quadratic of CA/CHI and SDS concentration and the quadratic of CA/CHI and CHI/PEO were significant. However, the interaction between the CA/CHI and the quadratic

***Table 4: Predicted optimum conditions and responses for the formed ENFs.***

| Properties | Goal | Lower Limit | Upper Limit | Predicted value | Actual value |
|---|---|---|---|---|---|
| A:CA/CHI | is in range | 0.5 | 1.5 | 1.5 | 1.47 |
| B: CHI/PEO | is in range | 1 | 2 | 1 | 1.02 |
| C: SDS | is in range | 0 | 3 | 3 | 2.74 |
| FD | Minimize | 89 | 119 | 95 | 96.08 |
| PO | Maximize | 37.11 | 75.18 | 52.68 | 52.29 |
| TS | Maximize | 0.01 | 0.06 | 0.058 | 0.05 |
| EL | Maximize | 5.82 | 19.55 | 12.87 | 13.09 |

of CHI/PEO were not significant. The most significant effect on diameter value was revealed to be a linear effect of SDS concentration, the quadratic effect of CA/CHI ratio and SDS concentration, the interaction among the ratio of CA/CHI & CHI/PEO and SDS concentration, the interaction between the quadratic of CA/CHI and SDS concentration and the quadratic of CA/CHI and CHI/PEO concentration. In the fitted model, $R^2$, adj-$R^2$, pred-$R^2$, CV and ADP values were 0.996, 0.95, 0.81, 0.75, and 45.04 respectively. Multiple regression analysis was applied to construct the Cubic model and equation obtained by conversion relating extent to the variables coded levels were:

$$\text{Diameter (nm)} = 101.418-3X_1-3X2+7.5X_3-1.875X_1X_2-3.125X_1X_3+1.375X_2X_3\ \ 5.045X_{12}+9.454X_{32}-2.375X_1X_2X_3+2.875X_{12}X_2-13.375X_{12}X_3$$

The outcomes revealed that the ratio of CA/CHI, CHI/PEO, and SDS content strongly affected the morphology and structure of the ENFs. An increase in the PEO concentration of the solutions can increase the fiber diameters due to raising the higher molecular weight, *Baek et al*. [18] reported that PEO increased in polymer chain entanglement and *Broumand et al.* [30] also determined that the high molecular weight of PEO (Mn = 200 kDa) has a high impact on the size of ENFs. According to table 3, the fiber diameter of blended fiber CA/CHI/PEO is lower than CA/PEO and higher than CHI/PEO nanofibers.

***RSM optimization***

Diameter, porosity, and mechanical strength as three important factors that were analyzed due to the fabrication of high-qualified ENFs in this study. It illustrates in Fig.1 that the distribution of the majority ENFs is homogenous. The optimization of independent variables was carried out by the presented information in table 4. The suggested optimum conditions examined the accuracy of polynomial regression equations to predict optimum responses (CA/CHI of 1.5%, CHI/PEO 1%, and SDS 3%, w/w %) by repeating threefold for the independent variable.

***Predictive Validation models***

Validation is an excellent procedure to investigate the effectiveness of the model. The confirmation experiments illustrated that there is an excellent agreement between actual experimental data and predicted one (Table 4). The equations of the model implied the great potential to determine the parameters for forming an appropriate electrospun nanofiber structure.

**CONCLUSIONS**

Fabrication of cellulose–chitosan hybrid nanofibers with acetic acid as a solvent was carried out by two approaches using electrospinning and making a solution by introducing chitosan directly to CA solution. Moreover, PEO was introduced to interfere actively with CA and CHI through hydrogen bonding on the molecular level and SDS and ammonium oxalate was added to decrease the surface tension and improve the conductivity. As was observed, an increase in CA/CHI, CHI/PEO, and SDS concentration led to a decrease in the diameter of the nanofiber. This research showed that CA increased the strength of blended nanofibers and chitosan improved its elongation of it because of having flexible fiber. The blended CA/CHI/PEO nanofibers showed the highest elongation and tensile strength among CA/PEO and CHI/PEO nanofibers and smaller diameter sizes and porosity percentage toward CA/PEO. This effective electrospinning procedure of chitosan-cellulose acetate mixtures produced

nanofibers with the range of 89–119 nm diameters at the fixed 4.8% w/v CA/CHI/PEO polymer concentration, which made uniform bead-free fibers. Moreover, the concentration of the solution is an important parameter to control the fiber morphology, which is influenced by the amount and ratio of CHI/CA/PEO and SDS. The hybrid CA and CHI ENFs have higher active sites in primary amine (-$NH_2$) and hydroxyl (-OH) groups. Hence, it is suggested that applying this blended fiber with a great potential for immobilization enzymes, and food packaging, and absorbing heavy metals of water.

*Received : Jun. 22, 2021 ; Accepted : Sep. 20, 2021*

## REFERENCES


[1] Liu G., Ding J., Qiao L., Guo A., Dymov B.P., Gleeson J.T., Hashimoto T., Saijo K., Polystyrene-block- poly (2- cinnamoylethyl methacrylate) Nanofibers-Preparation, Characterization, and Liquid Crystalline Properties, *Chem. Eur. J.*, **5(9)**: 2740-2749 (1999).

[2] Feng L., Li S., Li H., Zhai, J., Song Y., Jiang L., Zhu D, Super- hydrophobic Surface of Aligned Polyacrylonitrile Nanofibers, *Angew. Chem., Int. Ed. Engl*., **41(7)**: 1221-1223 (2002).

[3] Deitzel J.M., Kleinmeyer J., Hirvonen J.K., Beck T.N.C., Controlled Deposition of Electrospun Poly(ethylene oxide) Fibers, *Polymer*, **42**:8163–70 (2001).

[4] Ondarcuhu T., Joachim C., Drawing a Single Nanofibre over Hundreds of Microns, *EPL (Europhysics Letters)*, **42(2)**: 215 (1998).

[5] Ma P.X., Zhang R., Synthetic Nano- Scale Fibrous Extracellular Matrix, *J Biomed Mater Res B Appl Biomater*, **46(1)**: 60-72 (1999).

[6] Huang W., Xu H., Xue Y., Huang R., Deng H., Pan S., Layer-by-Layer Immobilization of Lysozyme–Chitosan–Organic Rectorite Composites on Electrospun Nanofibrous Mats for Pork Preservation, *Food Res. Int*., **48(2)**: 784 (2012).

[7] Demirkan E., Avci T., Aykut Y., Protease Immobilization on Cellulose Monoacetate/Chitosan-Blended Nanofibers, *J. Ind. Text*., **47(8)**: 2092 (2018).

[8] Jahani H., Jalilian F.A., Wu C.Y., Kaviani S., Soleimani M., Abbasi N., Hosseinkhani H., Controlled Surface Morphology and Hydrophilicity of Polycaprolactone Toward Selective Differentiation of Mesenchymal Stem Cells to Neural Like Cells, *J. Biomed. Mater. Res. A*, **103(5)**: 1875-1881 (2015).

[9] Khoshraftar A., Noorani B., Yazdian F., Rashedi H., Vaez Ghaemi R., Alihemmati Z., Shahmoradi S., Fabrication and Evaluation of Nanofibrous Polyhydroxybutyrate Valerate Scaffolds Containing Hydroxyapatite Particles for Bone Tissue Engineering, *Int. J. Polym. Mater*., **67(17)**: 987-995 (2018).

[10] Shahmoradi S., Golzar H., Hashemi M., Mansouri V., Omidi M., Yazdian F., Tayebi L., Optimizing the Nanostructure of Graphene Oxide/Silver/Arginine for Effective Wound Healing, *Nanotechnology*, **29(47)**: 475101(2018).

[11] Sundarrajan S., Tan K.L., Lim S.H. Ramakrishna S., Electrospun Nanofibers for Air Filtration Applications, *Procedia Eng.*, **75**: 159 (2014).

[12] Lee K.Y., Jeong L., Kang Y.O., Lee S.J., Park W.H., Electrospinning of Polysaccharides for Regenerative Medicine, *Drug Deliv. Rev.*, **61(12)**: 1020 (2009).

[13] Liu Z., Wang H., Li B., Liu C., Jiang Y., Yu G., Mu X., Biocompatible Magnetic Cellulose–Chitosan Hybrid Gel Microspheres Reconstituted from Ionic Liquids for Enzyme Immobilization, *J. Mater. Chem.*, **22(30)**: 15085 (2012).

[14] Kim C.W., Kim D.S., Kang S.Y., Marquez M., Joo Y.L., Structural Studies of Electrospun Cellulose Nanofibers, *Polymer (Guildf)*, **47(14)**: 5097 (2006).

[15] Kim S.J., Lee C.K., Kim S.I., Effect of Ionic Salts on the Processing of Poly (2- acrylamido- 2- methyl- 1- propane sulfonic acid) Nanofibers, *J. Appl. Polym. Sci*, **96(4)**: 1388 (2005).

[16] Li N., Bai R., Copper Adsorption on Chitosan–Cellulose Hydrogel Beads: Behaviors and Mechanisms, *Purif. Technol*., **42(3)**: 237(2005).

[17] Salihu G., Goswami P., Russell S., Hybrid Electrospun Nonwovens from Chitosan/Cellulose Acetate, *Cellulose*, **19(3)**: 739 (2012).

[18] Baek W.I., Pant H.R., Nam K.T., Nirmala R., Oh H.J., Kim I., Kim H.Y., Effect of Adhesive on the Morphology and Mechanical Properties of Electrospun Fibrous Mat of Cellulose Acetate, *Carbohydr. Res*, **346(13)**: 1956 (2011).

[19] Du J., Hsieh Y.L., Cellulose/Chitosan Hybrid Nanofibers from Electrospinning of Their Ester Derivatives, *Cellulose*, **16(2)**: 247 (2009).

[20] Fakirov S., "Fundamentals of Polymer Science for Engineers". Wiley-VCH (2017).

[21] Broumand A., Emam-Djomeh, Z., Khodaiyan F., Mirzakhanlouei S., Davoodi D., Moosavi-Movahedi, A.A., Nano-Web Structures Constructed with a Cellulose Acetate/Lithium Chloride/Polyethylene Oxide Hybrid: Modeling, Fabrication and Characterization, *Carbohydr. Polym.*, **115**: 760 (2015).

[22] Ghasemi- Mobarakeh L., Semnani D. and Morshed, M., A Novel Method for Porosity Measurement of Various Surface Layers of Nanofibers Mat Using Image Analysis for Tissue Engineering Applications, *J. Appl. Polym. Sci.*, **106(4)**: 2536 (2007).

[23] Zhang L., Hsieh Y.L., Ultra-Fine Cellulose Acetate/Poly (Ethylene Oxide) Bicomponent Fibers, *Carbohydr. Polym.*, **71(2)**: 196 (2008).

[24] Gharibzahedi S.M.T., Mousavi S.M., Khodaiyan F., Hamedi M., Optimization and Characterization of Walnut Beverage Emulsions in Relation to their Composition and Structure, *J. Biol. Macromol.*, **50(2)**: 376 (2012).

[25] Myers R.H., Montgomery D.C., Vining G.G., Borror C.M., Kowalski S.M., Response Surface Methodology: A Retrospective and Literature Survey, *J. Qual. Technol.*, **36(1)**: 53(2004).

[26] Jung Y.J., An B.J., Choi H.W., Kim H.S., Lee Y.H., Preparation and Characterization of Chitosan/ Cellulose Acetate Blend Film, *Text Coloration Finish*, **19(4)**: 10-17 (2007).

[27] Kriegel C., Arrechi A., Kit K., McClements D.J., Weiss J., Fabrication, functionalization, and Application of Electrospun Biopolymer Nanofibers, *Crit. Rev. Food Sci. Nutr.*, **48(8)**: 775 (2008).

[28] Jia L., Qin X.H., The Effect of Different Surfactants on the Electrospinning Poly (Vinyl Alcohol) (PVA) Nanofibers, *J. Therm. Anal. Calorim.*, **112(2)**: 595 (2013).

[29] Rosen M.J., Kunjappu J.T., "Surfactants and Interfacial Phenomena", John Wiley & Sons, Inc. (2012).

[30] Broumand A., Emam-Djomeh Z., Khodaiyan F., Davoodi D., Mirzakhanlouei, S., Optimal Fabrication of Nanofiber Membranes from Ionized-Bicomponent Cellulose/Polyethyleneoxide Solutions, *Int. J. Biol. Macromol.*, **66**: 221(2014).